J Physiol Sci (2017) 67:325–330
DOI 10.1007/s12576-016-0466-z

ORIGINAL PAPER

Changes in effective diffusivity for oxygen during neural activation and deactivation estimated from capillary diameter measured by two-photon laser microscope

Hiroshi Ito[1,2] · Hiroyuki Takuwa[1] · Yosuke Tajima[1] · Hiroshi Kawaguchi[1,3] · Takuya Urushihata[1] · Junko Taniguchi[1] · Yoko Ikoma[1] · Chie Seki[1] · Masanobu Ibaraki[4] · Kazuto Masamoto[1,5] · Iwao Kanno[1]

Received: 14 January 2016 / Accepted: 14 June 2016 / Published online: 25 June 2016

Abstract The relation between cerebral blood flow (CBF) and cerebral oxygen extraction fraction (OEF) can be expressed using the effective diffusivity for oxygen in the capillary bed (D) as $\mathrm{OEF} = 1 - \exp(-D/\mathrm{CBF})$. The D value is proportional to the microvessel blood volume. In this study, changes in D during neural activation and deactivation were estimated from changes in capillary and arteriole diameter measured by two-photon microscopy in awake mice. Capillary and arteriole vessel diameter in the somatosensory cortex and cerebellum were measured under neural activation (sensory stimulation) and neural deactivation [crossed cerebellar diaschisis (CCD)], respectively. Percentage changes in D during sensory stimulation and CCD were 10.3 ± 7.3 and -17.5 ± 5.3 % for capillary diameter of <6 μm, respectively. These values were closest to the percentage changes in D calculated from previously reported human positron emission tomography data. This may indicate that thinner capillaries might play the greatest role in oxygen transport from blood to brain tissue.

✉ Hiroyuki Takuwa
takuwa@nirs.go.jp

[1] Biophysics Program, Molecular Imaging Center, National Institute of Radiological Sciences, 4-9-1 Anagawa, Inage-ku, Chiba 263-8555, Japan

[2] Advanced Clinical Research Center, Fukushima Medical University, Fukushima, Japan

[3] Human Informatics Research Institute, National Institute of Advanced Industrial Science and Technology, Tsukuba, Japan

[4] Department of Radiology and Nuclear Medicine, Akita Research Institute of Brain and Blood Vessels, Akita, Japan

[5] Center for Frontier Science and Engineering, University of Electro-Communications, Chofu, Tokyo, Japan

Keywords Brain imaging · Capillary · Cerebral blood flow · PET · Two-photon laser microscope

Introduction

It is well known that cerebral blood flow (CBF) is essential to maintain brain metabolism. The relationship between CBF and cerebral metabolic rate of oxygen ($\mathrm{CMRO_2}$) is expressed as $\mathrm{CMRO_2} = \mathrm{CBF} \times \mathrm{OEF} \times \mathrm{Ca}$, where OEF is the oxygen extraction fraction and Ca is the total oxygen content in arterial blood. According to the model for the regulation of cerebral oxygen delivery proposed by Hyder et al. [1], OEF can be expressed using the effective diffusivity for oxygen in the capillary bed (D) as $\mathrm{OEF} = 1 - \exp(-D/\mathrm{CBF})$. It follows that $\mathrm{CMRO_2}$ can be written as $\mathrm{CBF} \times \mathrm{Ca} \times (1 - \exp(-D/\mathrm{CBF}))$. Even though the biological processes controlling D remain unclear, in previous work using Hyder's model and two-photon imaging of animal cerebral vasculature, we have shown that D is closely associated with diameter changes of cerebral microvessels [2, 3]. As oxygen transport from blood to brain tissue is mainly performed in the capillaries [4, 5], it is possible that change in D can be estimated from changes in capillary diameter.

The discrepancy between changes in CBF and $\mathrm{CMRO_2}$ during neural activation and deactivation is well known [6–8]. This discrepancy causes changes in OEF and therefore changes in blood oxygenation level-dependent (BOLD) contrast for functional magnetic resonance imaging (fMRI) [9, 10]. Previously, we reported the increases in CBF and decrease in OEF during neural activation caused by a motor task [10], and the decrease in CBF and increase in OEF during neural deactivation observed in crossed cerebellar diaschisis (CCD) caused by contralateral supratentorial

lesions [9] using positron emission tomography (PET) in humans. According to these results, changes in D during neural activation and deactivation can be estimated.

In the present study, changes in D during neural activation and deactivation were estimated from changes in diameter of capillaries and thin arterioles measured from in vivo two-photon laser microscopic imaging in awake mice, and they were compared with those calculated from measures by PET in humans reported previously. Neural activation was introduced in the barrel cortex by whisker stimulation [11, 12]. Neural deactivation was introduced in the cerebellar cortex by CCD after onset of cerebral infarction due to middle cerebral artery occlusion (MCAO) [13].

Materials and methods

Animal preparation

All experiments were performed in accordance with the institutional guidelines on the humane care and use of laboratory animals and were approved by the Institutional Committee for Animal Experimentation. Six male C57BL/6J mice (20–30 g, 7–11 weeks; Japan SLC Inc., Hamamatsu, Japan) were used in the two-photon imaging experiment. The animals were housed in a 12-h light/dark cycle room at a temperature of 25 °C with ad libitum water and food.

For the surgical procedure, the animals were anesthetized with a mixture of air, oxygen and isoflurane (3 % for induction and 2 % for surgery) via facemask. The animals were fixed in a stereotactic frame, and rectal temperature was maintained at 37.0 °C using a heating pad (ATC-210, Unique Medical Co. Ltd., Tokyo, Japan). The methods for preparing the chronic cranial window have been reported in detail previously [2, 14]. A midline incision (10 mm) was made to expose the skull. Two cranial windows were attached over the left side of the cerebral cortex (approximately 3-mm diameter, centered at 1.8 mm caudal and 2.5 mm lateral from bregma) and over the right side of the cerebellar cortex (coordinates: 1 mm posterior from the occipital bone, 4 mm lateral), keeping the dura intact. A custom metal plate was affixed to the front of the skull using dental cement (Ionosit, DMG, Hamburg, Germany). After completion of the surgery, the animals were allowed to recover from anesthesia and housed for at least 14 days before initiation of the experiments.

Two-photon imaging experiment

Sulforhodamine 101 (SR101; MP Biomedicals, Irvine, CA, USA) dissolved in saline (10 mM) was injected intraperitoneally (SR101: 8 µl/g body weight) just before the start of the imaging experiments. The awake animal was placed on a custom-made apparatus [11], and imaging was conducted using a two-photon microscope (TCS-SP5 MP, Leica Microsystems GmbH, Wetzlar, Germany) with an excitation of 900 nm. An emission signal was detected through a band-pass filter for SR101 (610/75 nm). A single image plane consisted of 1024 × 1024 pixels, and the in-plane pixel-size was 0.2 µm. Volume images were acquired up to a maximum depth of 0.4 mm from the cortical surface with a z-step size of 2.5 µm [15].

Whisker stimulation (neural activation)

The methods for dynamic two-photon imaging of vasodilation have been reported in detail previously [16]. Briefly, dynamic imaging was conducted in capillaries and arterioles of the barrel cortex at a rate of 0.15 s per frame for 20 s (i.e., 5-s pre-stimulus, 5-s stimulus, and 10-s post-stimulus). A total of either 3 or 5 trials were repeatedly performed with an inter-trial interval of 30 s, and the image was averaged over the trials to improve the signal-to-noise ratio. After the two-photon imaging experiment, the diameters of the blood vessels were measured offline with LAS AF software (Leica Microsystems GmbH, Wetzlar, Germany). To measure the diameter of a blood vessel, we chose a region of interest on a single vessel segment between two branch points. Between four and nine such measurements on different capillaries and arterioles were made for each mouse, and then averaged. The average diameter of the capillaries and arterioles was estimated from 5-s pre-stimulus periods (baseline) and 1–6 s after whisker stimulation for vessel type, i.e., <6 µm (capillary), 6–10 µm (capillary), and 10–15 µm (arteriole). We defined vessels with a diameter of 10–15 µm to be arterioles because 10–15-µm-thick cortical microvessels in the mouse brain are surrounded by smooth muscle cells [17].

The experimental protocol for whisker stimulation has been reported previously [2]. In whisker stimulation, compressed air (up to 10 psi) controlled with a Pico Pump (PV830, WPI, Osaka, Japan) was delivered to the entire right whisker region. A 5-s rectangular pulse stimulation (50-ms pulse width and 100-ms onset-to-onset interval, i.e., 10 Hz frequency) was generated with a Master-8 (A.M.P.I, Jerusalem, Israel).

Crossed cerebellar diaschisis (neural deactivation)

MCAO was performed by Tamura et al.'s [18] method. Briefly, permanent occlusion was made at the proximal branch of the MCA in the left cerebral cortex. Thus, the right and left sides of the cerebellar cortex were defined as CCD side and unaffected side, respectively [13]. Two-

photon imaging experiments were performed in the CCD side of the cerebellar cortex before (baseline) and 1 day after MCAO. Static imaging was conducted in capillaries of the cerebellar cortex. After the two-photon imaging experiment, diameters of the blood vessels were measured offline with LAS AF software (Leica Microsystems GmbH, Wetzlar, Germany). The average diameter of the capillaries and arterioles was calculated at baseline and 1 day after MCAO for each range of diameter, i.e., <6, 6–10, and 10–15 μm.

Calculation of changes in effective diffusivity for oxygen from capillary diameter

The percentage changes in capillary diameter from baseline were calculated for whisker stimulation and CCD, and statistical analyses by paired *t*-test were performed to compare the vessel diameters between baseline and whisker stimulation or CCD. Because effective diffusivity for oxygen in the capillary bed *D* is proportional to the capillary and thin arterioles volume corresponding to the square of the vessel diameter if capillary length does not change [1], the percentage changes in the square of the vessel diameter from baseline were calculated for whisker stimulation and CCD as the percentage changes in *D* for each range of diameter, i.e., <6, <10, and <15 μm. We performed statistical analysis to compare *D* across the three vessel groups using one-way ANOVA followed by the Tukey–Kramer test.

Results

The cortical capillary vessels imaged by two-photon laser microscope through a chronic cranial window in the barrel cortex and the cerebellar cortex are shown in Fig. 1. Capillary and arteriole diameters in the barrel cortex at baseline and during whisker stimulation are shown in Table 1. Significant increases in vessel diameters during whisker stimulation were observed for each range of vessel diameter. Capillary and arteriole diameters in the cerebellar cortex at baseline and during CCD are shown in Table 2. Significant decreases in vessel diameters during CCD were observed for each range of capillary diameter. Percentage changes in capillary diameters during whisker stimulation and CCD are also shown in Tables 1 and 2. When the vessel diameter was smaller, absolute values of percentage changes in capillary diameter during both whisker stimulation and CCD were smaller.

Table 1 Capillary diameter in barrel cortex at baseline and during whisker stimulation, and percentage changes in capillary diameter during whisker stimulation for each range of capillary diameter

	Baseline (μm)	Whisker stimulation (μm)	% Change
<6 μm	4.63 ± 0.55	4.88 ± 0.72*	5.0 ± 3.5
6–10 μm	7.50 ± 0.70	8.35 ± 0.96*	11.4 ± 6.3
10–15 μm	12.43 ± 0.87	14.33 ± 1.30*	15.2 ± 4.9

Values are mean ± SD

Significant differences from baseline (paired *t*-test): * $P < 0.05$

Percentage changes in effective diffusivity for oxygen *D* during whisker stimulation and CCD are shown in Table 3. When the vessel diameter was smaller, absolute values of percentage changes in *D* during both whisker stimulation and CCD were smaller. There is a significant difference in *D* between vessels with diameter < 6 μm and vessels with diameter 10–15 μm ($P < 0.05$) (Table 3).

Discussion

In the present study, significant increases and decreases in capillary and arteriole diameter during neural activation and deactivation were observed, and the estimated

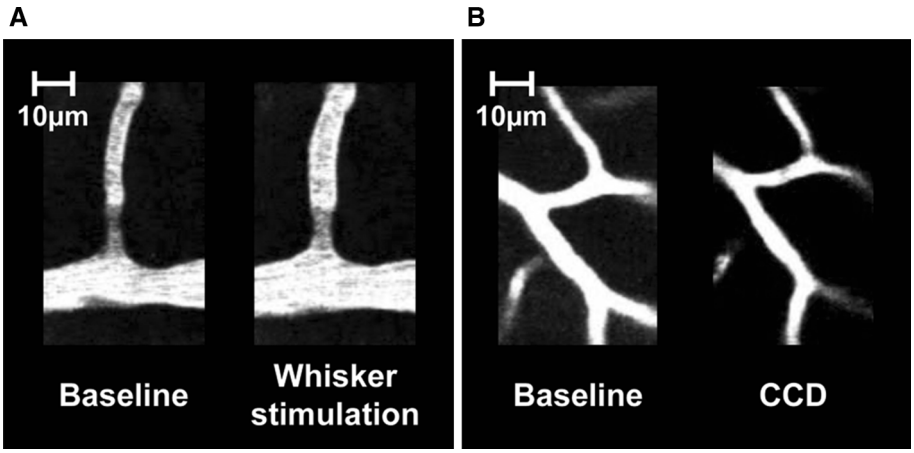

Fig. 1 The cortical capillary vessels imaged by two-photon laser microscope through a chronic cranial window at baseline and during whisker stimulation in barrel cortex (**a**) and at baseline and during crossed cerebellar diaschisis (CCD) in cerebellar cortex (**b**)

Table 2 Capillary diameter in cerebellar cortex at baseline and during crossed cerebellar diaschisis (CCD), and percentage changes in capillary diameter during CCD for each range of capillary diameter

	Baseline (μm)	CCD (μm)	% Change
<6 μm	5.01 ± 0.28	4.55 ± 0.35*	−9.2 ± 2.9
6–10 μm	7.22 ± 0.51	6.35 ± 0.60*	−12.0 ± 6.1
10–15 μm	11.88 ± 0.85	10.34 ± 0.73*	−12.7 ± 7.3

Values are mean ± SD

Significant differences from baseline (paired *t*-test): * $P < 0.05$

Table 3 Percentage changes in effective diffusivity for oxygen D during whisker stimulation and crossed cerebellar diaschisis (CCD) for each range of capillary diameter

	Whisker stimulation (%)	CCD (%)
<6 μm	10.3 ± 7.3*	−17.5 ± 5.3
<10 μm	19.1 ± 8.5	−20.5 ± 5.8
<15 μm	26.3 ± 8.2*	−22.1 ± 7.4

Values are mean ± SD

Significant differences (ANOVA): * $P < 0.05$

effective diffusivity for oxygen D showed corresponding increases and decreases during neural activation and deactivation, respectively. The absolute percentage changes in D during both neural activation and deactivation were smaller when the capillary and arteriole diameters were smaller. To compare the D value between this study and a human PET study, we estimated D from human PET data collected in previous studies [9, 10]. The D value was calculated as $\mathrm{OEF} = 1 - \exp(-D/\mathrm{CBF})$, and the percentage change in D during neural activation was calculated from D values at baseline and during the motor task. Using the mean values of the CBF and OEF in the primary motor cortex at baseline and during a motor task (baseline: CBF = 57 ml/100 ml/min, OEF = 0.34; motor task: CBF = 84 ml/100 ml/min, OEF = 0.26) [10], the calculated percentage change in D during neural activation was estimated to be 6.8 % (baseline: $D = 0.237$ ml/ml/min; motor task: $D = 0.253$ ml/ml/min). For neural deactivation, the percentage change in D during neural deactivation was calculated with the unaffected side acting as the baseline. Using the mean values for CBF and OEF in both the CCD and unaffected sides of the cerebellar cortex previously reported with PET (CCD side: CBF = 41 ml/100 ml/min, OEF = 0.42; unaffected side: CBF = 51 ml/100 ml/min, OEF = 0.39) [9], the estimated percentage change in D during neural deactivation (using the unaffected side as baseline) was −11.4 % (CCD side: $D = 0.223$ ml/ml/min; unaffected side: $D = 0.252$ ml/ml/min). For a capillary diameter of < 6 μm, the percentage changes in D during both neural activation and deactivation were closest to the percentage changes in D calculated from the previously reported human PET data. This may indicate that thinner capillaries play a greater role in oxygen transport from blood to brain tissue. A linear relation between red blood cell (RBC) velocity and capillary diameter has been reported [5, 19]. Since the RBC velocity is slow in thin capillaries, the long transit time of RBC in thin capillaries may allow the transport of sufficient oxygen. In addition, a proportional relation between capillary transit time and OEF has been reported [20]. The diameter of mouse RBC has been reported as about 6 μm [21]. Thus, RBCs are near the wall of capillaries with a diameter under 6 μm, allowing the transport of enough oxygen. On the other hand, it has also been reported that all microvessels, including arterioles, capillaries, and venules contribute to the supply of oxygen to brain tissue [22].

Although the degree of changes in D during both neural activation and deactivation was greater in the estimation with mouse capillary diameter than in the estimation with human PET data, the degree of changes in D during neural activation was less than during neural deactivation for both mice and humans. This also might indicate the validity of the model for the regulation of cerebral oxygen delivery proposed by Hyder et al. [1].

In making the above comparison between human and mouse estimates for D, it should be remembered that the mouse value was calculated from microvessel diameter measurement, while the human value came from PET data. To verify whether the comparison is valid, D could be estimated from mouse PET data in a future study.

The capillary diameter changes with alterations in CBF in relation to neural activity. Several factors regarding the control of capillary blood flow in the brain have been proposed, i.e., intravascular factors including RBC, vascular factors including endothelial cells and pericytes, and parenchymal factors including neurons and astrocytes [23]. Two main mechanisms of changes in capillary diameter during neural activation and deactivation should be considered. One is passive changes in capillary diameter depending on perfusion pressure regulated by the precapillary arteriole. Another is the active control of capillary diameter by pericytes [24, 25]. Although it is unknown whether the mechanism of changes in capillary diameter is passive or active, according to Hyder's model, the D value can be proportional to capillary blood volume for the regulation of cerebral oxygen delivery [1].

Because the D value is proportional to the capillary volume [1], changes in capillary density as well as capillary diameter can also introduce changes to the D value. However, increases in capillary blood velocity, not in capillary blood volume, were observed during neural activation [26] or hypercapnia [27], indicating no capillary recruitment. In this study, no changes in the number of

capillary vessels during neural activation and deactivation were observed by two-photon laser microscopic imaging. This might also indicate that there was no capillary recruitment. On the other hand, increases in capillary blood velocity during neural activation [26] or hypercapnia [27] were accompanied by a decrease in heterogeneity of blood velocity of each capillary vessel. Such RBC recruitment during neural activation might also be related to changes in *D* value. In addition, we have reported changes in RBC concentration during neural activation and deactivation as measured by laser-Doppler flowmetry in awake mice to be about 2 and 20 %, respectively [12, 13]. Such changes might affect changes in *D* [28]. However, since the RBC concentration measured by laser-Doppler flowmetry includes all components of cerebral vessels, i.e., artery, capillary, and vein, further studies to determine changes in capillary RBC concentration during neural activation and deactivation will be required. In addition, no significant changes in hematocrit during neural activation were observed [29].

In conclusion, changes in *D* during neural activation and deactivation were estimated from changes in capillary diameter measured by two-photon imaging in awake mice, and compared with those calculated from measures by PET in humans according to Hyder's model for the regulation of cerebral oxygen delivery. When the capillary diameter was smaller, absolute values of percentage changes in *D* during both neural activation and deactivation were smaller and closest to the percentage changes in *D* calculated from human PET data. This would indicate that thinner capillaries might play the greatest role in oxygen transport from blood to brain tissue.

Acknowledgments The assistance of members of the National Institute of Radiological Sciences in performing the two-photon laser microscope experiments is gratefully acknowledged. We would also like to thank Jeff Kershaw for his assistance in refining the manuscript.

Compliance with ethical standards

Conflict of interest The authors report no conflicts of interest.

References

1. Hyder F, Shulman RG, Rothman DL (1998) A model for the regulation of cerebral oxygen delivery. J Appl Physiol 85:554–564
2. Takuwa H, Masamoto K, Yamazaki K, Kawaguchi H, Ikoma Y, Tajima Y et al (2013) Long-term adaptation of cerebral hemodynamic response to somatosensory stimulation during chronic hypoxia in awake mice. J Cereb Blood Flow Metab 33:774–779
3. Tajima Y, Takuwa H, Kokuryo D, Kawaguchi H, Seki C, Masamoto K et al (2014) Changes in cortical microvasculature during misery perfusion measured by two-photon laser scanning microscopy. J Cereb Blood Flow Metab 34:1363–1372
4. Masamoto K, Tanishita K (2009) Oxygen transport in brain tissue. J Biomech Eng 131:074002
5. Safaeian N, David T (2013) A computational model of oxygen transport in the cerebrocapillary levels for normal and pathologic brain function. J Cereb Blood Flow Metab 33:1633–1641
6. Fox PT, Raichle ME (1986) Focal physiological uncoupling of cerebral blood flow and oxidative metabolism during somatosensory stimulation in human subjects. Proc Natl Acad Sci USA 83:1140–1144
7. Seitz RJ, Roland PE (1992) Vibratory stimulation increases and decreases the regional cerebral blood flow and oxidative metabolism: a positron emission tomography (PET) study. Acta Neurol Scand 86:60–67
8. Vafaee MS, Gjedde A (2000) Model of blood–brain transfer of oxygen explains nonlinear flow-metabolism coupling during stimulation of visual cortex. J Cereb Blood Flow Metab 20:747–754
9. Ito H, Kanno I, Shimosegawa E, Tamura H, Okane K, Hatazawa J (2002) Hemodynamic changes during neural deactivation in human brain: a positron emission tomography study of crossed cerebellar diaschisis. Ann Nucl Med 16:249–254
10. Ito H, Ibaraki M, Kanno I, Fukuda H, Miura S (2005) Changes in cerebral blood flow and cerebral oxygen metabolism during neural activation measured by positron emission tomography: comparison with blood oxygenation level-dependent contrast measured by functional magnetic resonance imaging. J Cereb Blood Flow Metab 25:371–377
11. Takuwa H, Autio J, Nakayama H, Matsuura T, Obata T, Okada E et al (2011) Reproducibility and variance of a stimulation-induced hemodynamic response in barrel cortex of awake behaving mice. Brain Res 1369:103–111
12. Takuwa H, Matsuura T, Obata T, Kawaguchi H, Kanno I, Ito H (2012) Hemodynamic changes during somatosensory stimulation in awake and isoflurane-anesthetized mice measured by laser-Doppler flowmetry. Brain Res 1472:107–112
13. Takuwa H, Tajima Y, Kokuryo D, Matsuura T, Kawaguchi H, Masamoto K et al (2013) Hemodynamic changes during neural deactivation in awake mice: a measurement by laser-Doppler flowmetry in crossed cerebellar diaschisis. Brain Res 1537:350–355
14. Tomita Y, Kubis N, Calando Y, Tran Dinh A, Meric P, Seylaz J et al (2005) Long-term in vivo investigation of mouse cerebral microcirculation by fluorescence confocal microscopy in the area of focal ischemia. J Cereb Blood Flow Metab 25:858–867
15. Park SH, Masamoto K, Hendrich K, Kanno I, Kim SG (2008) Imaging brain vasculature with BOLD microscopy: MR detection limits determined by in vivo two-photon microscopy. Magn Reson Med 59:855–865
16. Sekiguchi Y, Masamoto K, Takuwa H, Kawaguchi H, Kanno I, Ito H et al (2013) Measuring the vascular diameter of brain surface and parenchymal arteries in awake mouse. Adv Exp Med Biol 789:419–425
17. Hill RA, Tong L, Yuan P, Murikinati S, Gupta S, Grutzendler J (2015) Regional blood flow in the normal and ischemic brain is controlled by arteriolar smooth muscle cell contractility and not by capillary pericytes. Neuron 87:95–110
18. Tamura A, Graham DI, McCulloch J, Teasdale GM (1981) Focal cerebral ischaemia in the rat: 1. Description of technique and early neuropathological consequences following middle cerebral artery occlusion. J Cereb Blood Flow Metab 1:53–60
19. Hudetz AG (1997) Blood flow in the cerebral capillary network: a review emphasizing observations with intravital microscopy. Microcirculation 4:233–252
20. Jespersen SN, Ostergaard L (2012) The roles of cerebral blood flow, capillary transit time heterogeneity, and oxygen tension in brain oxygenation and metabolism. J Cereb Blood Flow Metab 32:264–277

21. Engstrom KG, Taljedal IB (1987) Altered shape and size of red blood cells in obese hyperglycaemic mice. Acta Physiol Scand 130:535–543
22. Vovenko E (1999) Distribution of oxygen tension on the surface of arterioles, capillaries and venules of brain cortex and in tissue in normoxia: an experimental study on rats. European journal of physiology 437:617–623
23. Itoh Y, Suzuki N (2012) Control of brain capillary blood flow. J Cereb Blood Flow Metab 32:1167–1176
24. Peppiatt CM, Howarth C, Mobbs P, Attwell D (2006) Bidirectional control of CNS capillary diameter by pericytes. Nature 443:700–704
25. Hamilton NB, Attwell D, Hall CN (2010) Pericyte-mediated regulation of capillary diameter: a component of neurovascular coupling in health and disease. Front Neuroenerg 21:2
26. Schulte ML, Wood JD, Hudetz AG (2003) Cortical electrical stimulation alters erythrocyte perfusion pattern in the cerebral capillary network of the rat. Brain Res 963:81–92
27. Kuschinsky W, Paulson OB (1992) Capillary circulation in the brain. Cerebrovasc Brain Metab Rev 4:261–286
28. Hayashi T, Watabe H, Kudomi N, Kim KM, Enmi J, Hayashida K et al (2003) A theoretical model of oxygen delivery and metabolism for physiologic interpretation of quantitative cerebral blood flow and metabolic rate of oxygen. J Cereb Blood Flow Metab 23:1314–1323
29. Herman P, Sanganahalli BG, Hyder F (2009) Multimodal measurements of blood plasma and red blood cell volumes during functional brain activation. J Cereb Blood Flow Metab 29:19–24